Reaction of *Escherichia coli* Cytochrome bo_3 with Substoichiometric Ubiquinol-2: A Freeze-Quench Electron Paramagnetic Resonance Investigation†

Brian E. Schultz,‡ Dale E. Edmondson,§ and Sunney I. Chan*,‡

Division of Chemistry and Chemical Engineering, Arthur Amos Noyes Laboratory of Chemical Physics, California Institute of Technology, Pasadena, California 91125, and Departments of Biochemistry and Chemistry, Emory University, Atlanta, Georgia 30322

Received July 14, 1997; Revised Manuscript Received January 14, 1998

ABSTRACT: The reaction of the quinol oxidase cytochrome bo_3 from *Escherichia coli* with ubiquinol-2 (UQ_2H_2) was carried out using substoichiometric (0.5 equiv) amounts of substrate. Reactions were monitored through the use of freeze-quench EPR spectroscopy. Under 1 atm of argon, semiquinone was formed at the Q_B site of the enzyme with a formation rate constant of 140 s^{-1}; the Q_B semiquinone EPR signal decayed with a rate constant of about 5 s^{-1}. Heme *b* and Cu_B were reduced within the 10-ms dead time of the freeze-quench experiment and remained at a constant level of reduction over the 1-s time course of the experiment. Quantitation of the reduction levels of Q_B and heme *b* during this reaction yielded a reduction potential of 30−60 mV for heme *b*. Under a dioxygen atmosphere, the rates of semiquinone formation and its subsequent decay were not altered significantly. However, accurate quantitation of the EPR signals for heme *b* and heme o_3 could not be made, due to interference from dioxygen. In the reaction between the Q_B-depleted enzyme and UQ_2H_2 under substoichiometric conditions, there was no observable change in the EPR spectra of the enzyme over the time course of the reaction, suggesting an electron transfer from heme *b* to the binuclear site in the absence of Q_B which occurs within the dead time of the freeze-quench apparatus. Analysis of the thermodynamics and kinetics of electron transfers in this enzyme suggests that a Q-cycle mechanism for proton translocation is more likely than a cytochrome *c* oxidase-type ion-pump mechanism.

Utilization of dioxygen as a terminal electron acceptor in the respiratory chain of both eukaryotic and prokaryotic organisms is accomplished in large part by the superfamily of heme−copper oxidases (*1*). These enzymes have evolved to couple this reduction of dioxygen with the generation of a proton gradient across the plasma or mitochrondrial membrane. Members of this superfamily are distinguished by a conserved subunit containing a high-spin heme, a low-spin heme, and a copper ion. The high-spin heme and copper ion form a binuclear site at which dioxygen reduction occurs; the low-spin heme is involved in electron transfer. These enzymes are divided into two classes, the cytochrome *c* oxidases and the quinol oxidases, on the basis of their electron donors.

The most thoroughly studied of the cytochrome *c* oxidases is the mitochondrial enzyme (*2*, *3*). It contains 13 subunits, of which subunits I−III are encoded by mitochondrial genes and the remaining 10 are encoded in nuclear genes. Subunit I contains the low-spin heme *a*, the high-spin heme a_3, and the mononuclear copper site (Cu_B). As with all other known cytochrome *c* oxidases with the exception of the cbb_3 enzymes, subunit II contains a binuclear copper center (Cu_A) in its extramembranous domain. Cytochrome *c* oxidase acts as an ion pump, transporting four protons through the enzyme over the course of the four-electron reduction of dioxygen to water.

The *Escherichia coli* cytochrome bo_3 complex, the best characterized of the quinol oxidases, is a four-subunit enzyme encoded by the *cyoABCDE* operon (*4*). In addition to a low-spin heme *b*, a high-spin heme o_3, and the Cu_B site in subunit I, this enzyme has been shown to possess a tightly bound molecule of UQ_8[1] at a site (Q_B) distinct from the site of quinol oxidation (Q_A) and in close proximity to heme *b* (*5*). From a functional standpoint, this enzyme combines the quinol oxidase function of cytochrome bc_1 with the dioxygen reduction capability of cytochrome *c* oxidase. However, cytochrome bo_3 is less efficient in generating a proton gradient than the cytochrome bc_1/cytochrome *c* oxidase system, translocating eight protons per four electrons (*6*) as compared to the $12H^+/4e^-$ ratio of the latter system.

The reaction of cytochrome *c* oxidase with dioxygen has been summarized elsewhere (*7*). To the extent that it has been determined, the sequence of intermediates arising during dioxygen reduction by cytochrome bo_3 appears to be identical to that of the cytochrome *c* oxidases. Saturation kinetics in

† This work was supported by Grants GM22432 (S.I.C.) and GM29433 (D.E.E.) from the National Institutes of Health. B.E.S. is the recipient of a National Science Foundation Postdoctoral Fellowship.

‡ California Institute of Technology.

§ Emory University.

[1] Abbreviations: DDM, *n*-dodecyl β-D-maltoside; DTT, dithiothreitol; HEPES, *N*-(2-hydroxyethyl)piperazine-*N*′-(2-ethanesulfonic acid); $Q_A(H_2)$, quinone(ol) in the quinol oxidation site of cytochrome bo_3; $Q_B(H_2)$, quinone(ol) in the alternative quinone binding site of cytochrome bo_3; TX-100, Triton X-100; UQ_n, ubiquinone (n = number of isoprenoid units in the hydrophobic side chain); UQ_nH_2, ubiquinol.

S0006-2960(97)01714-5 CCC: $15.00
Published on Web 03/05/1998

the binding of dioxygen to the high-spin hemes in both enzymes suggests the formation of an initial copper−dioxygen species (*8*). Flow-flash optical and resonance Raman studies have revealed intermediates in the dioxygen reduction chemistry assigned as the ferrous-oxy (compound A) (*9, 10*), peroxidic (compound C) (*11*), and oxyferryl (*8, 9*) species. Likewise, observed chemistry of cytochrome bo_3 with peroxide (*8, 11*−*15*) parallels that of cytochrome *c* oxidase, although the formation of the oxyferryl species is more highly favored in cytochrome bo_3. It should be noted, though, that the behavior of cytochrome bo_3 with respect to proton uptake during dioxygen reduction differs from that of cytochrome *c* oxidase (*16*).

The similarity of subunit I structure and the analogous dioxygen chemistry have led to the assumption that the proton translocation mechanisms are essentially identical between the cytochrome *c* oxidases and the quinol oxidases. This view assumes that the two hemes and Cu_B in subunit I are responsible for the proton translocation in both types of enzymes and that the presence of an additional redox center (Cu_A in cytochrome *c* oxidase and Q_B in cytochrome bo_3) serves the sole purpose of mediating the electron transfer from the electron donor to this catalytic core. However, a contrasting view has been put forward, suggesting that cytochrome bo_3 utilizes a Q-cycle analogous to that of cytochrome bc_1 (*17*). A recent study of inhibition of cytochrome bo_3 by substrate and by the semiquinone analogues 5-*n*-undecyl-6-hydroxy-4,7-dioxobenzothiazole (UHDBT) and 2-*n*-nonyl-4-hydroxyquinoline *N*-oxide (NQNO) has demonstrated that the Q_B quinone is exchangeable under turnover conditions, a necessary requirement for a Q-cycle mechanism, and that the affinities of sites Q_A and Q_B for quinols, semiquinones, and quinones are also in accord with a Q-cycle mechanism (*18*). However, these data cannot completely rule out an ion-pump mechanism for cytochrome bo_3.

Greater discrimination between the two mechanisms can be made on the basis of the electron transfer through the enzyme, as the electron-transfer pathways proposed by the two models are radically different. These models are shown schematically in Figure 1. An ion-pump mechanism for cytochrome bo_3 implies that the electron transfers through this enzyme are analogous to those in cytochrome *c* oxidases. In cytochrome *c* oxidase, studies using transient absorbance spectroscopy suggest that the flow of electrons from substrate to dioxygen occurs in the order cyt *c* → Cu_A → heme *a* → (heme a_3/Cu_B) (*19*). As no Cu_A site exists in cytochrome bo_3, the analogous electron transfers in this enzyme would be Q_AH_2 → heme *b* → (heme o_3/Cu_B). As Q_AH_2 is a two-electron donor while heme *b* is a one-electron redox center, electron transfer would require either the transient formation of the Q_A semiquinone or a split electron-transfer pathway in which one electron is passed to heme *b* and the second one is transferred elsewhere. Sato-Watanabe et al. (*5*) have postulated a split electron-transfer pathway, with the quinone in the Q_B site accepting the second electron. According to this model, electrons could then be transferred sequentially through heme *b* to the binuclear site. The release of four protons from the oxidation of two quinol molecules, along with the pumping of four protons during dioxygen reduction, would account for the observed proton translocation stoichiometry.

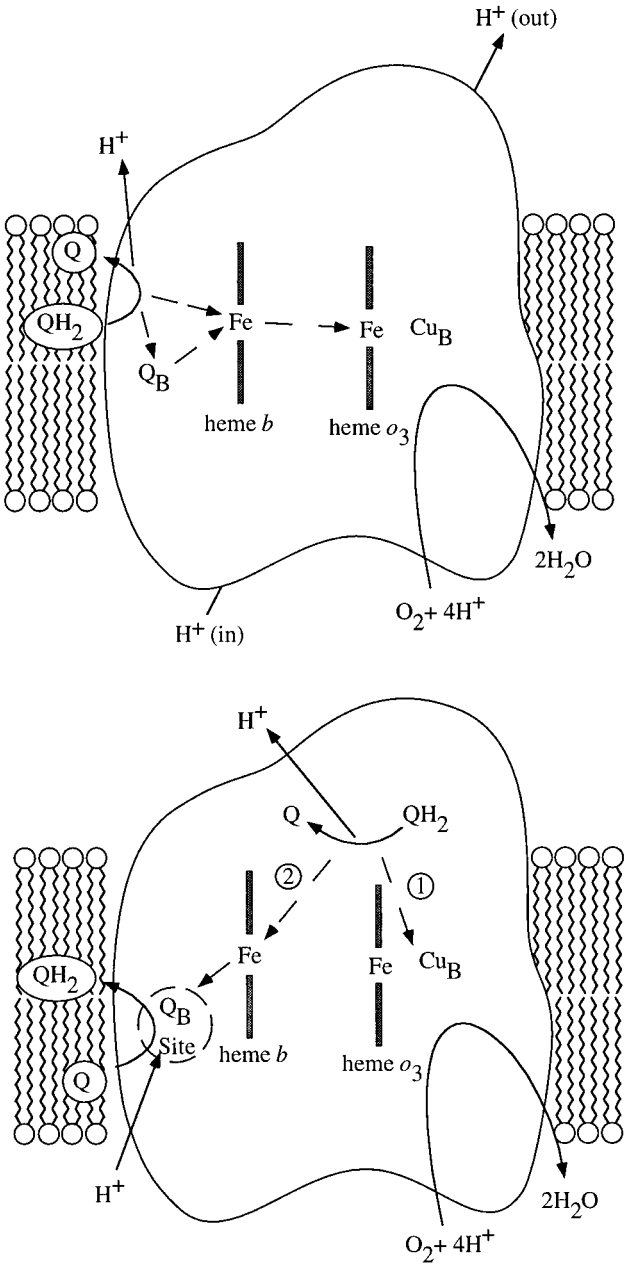

FIGURE 1: Schematic diagram of the proposed ion-pump (top) and Q-cycle (bottom) reaction mechanisms of cytochrome bo_3. Electron transfers are denoted by dashed lines. For the Q-cycle model, the numbers refer to the first and second electron transfers in the oxidation of quinol.

In analogy with the cytochrome bc_1 complex (*20, 21*), the Q-cycle hypothesis for cytochrome bo_3 postulates a split electron-transfer pathway in the oxidation of quinol, with one electron traveling to the high-potential Cu_B site and the other electron passing through heme *b* to reduce Q_B to its semiquinone form. Upon the oxidation of a second quinol, $Q_B^{\bullet}$ is reduced to a quinol, which can then dissociate and be replaced with another molecule of quinone. A complete turnover of the enzyme results in the oxidation of four quinol molecules with the associated release of eight protons on the outside of the plasma membrane, the reduction of two quinone molecules coupled with the uptake of four protons from the inside of the membrane, and the reduction of dioxygen to water. In this case, the observed $8H^+/4e^-$ proton-pumping ratio arises solely from quinol oxidation;

no ion pumping occurs, and the sole purpose of the binuclear heme−copper site is to act as an electron sink. Also, in contrast to the ion-pump model, this model suggests that electron transfer between heme *b* and heme o_3 is not important in the turnover process but that any adventitious electron-transfer represents an electron leak.

The viability of the electron-transfer pathways proposed in these two models depends on both the reduction potentials of the redox centers and the spatial arrangement of these centers. Understanding both the thermodynamics and kinetics of the electron transfers under turnover conditions requires a means to observe the reduction state of all of the redox centers in the protein. However, the most common methods used to monitor the reaction of cytochrome bo_3, optical absorption spectroscopy and resonance Raman spectroscopy, can only monitor the heme groups. We have chosen to probe the activity of the enzyme using rapid-mixing/freeze-quench EPR spectroscopy, as each of the four redox centers in cytochrome bo_3 has an oxidation state which is observable by this technique. The turnover number of cytochrome bo_3 in its reaction with UQ_2H_2 is approximately 1500 s^{-1} at room temperature, a rate which is rapid in comparison to the time scale of the freeze-quench experiment (10 ms or longer). To overcome this limitation, the freeze-quench reactions were performed at low temperature to slow the reaction, and the enzyme was reacted with a limited quantity of substrate. If the number of electrons entering the enzyme is limited, a complete enzyme turnover cycle cannot occur, the distribution of electrons within the enzyme can be determined, and electron transfers within the enzyme which occur on a nonphysiological time scale (e.g., electron leaks) can be monitored. The use of incomplete turnover conditions has allowed a meaningful measurement of the heme *b* potential under near-physiological conditions and has provided information on how this potential relates to electron transfers within the enzyme. The thermodynamic and kinetic data obtained in this study suggest that the electron transfers predicted by an ion-pump model are inconsistent with the observed data and that a Q-cycle mechanism is likely to be operating in this enzyme.

EXPERIMENTAL PROCEDURES

Reagents. HEPES, dithiothreitol, Triton X-100, *n*-octyl β-D-glucoside (Anatrace), and *n*-dodecyl β-D-maltoside (Anatrace) were from commercial sources and used as received. The synthesis of UQ_2H_2 will be described elsewhere.

Sample Preparation. *E. coli* (strain GO105/pJRHisA) cells were grown at the Univerisity of Illinois fermentation facility using a protocol described previously (*11*). "His-tagged" cytochrome bo_3 was isolated using the method of Musser and co-workers (*18*), with the following modifications: Following solubilization of the cytochrome bo_3 with DDM and *n*-octyl β-D-glucoside, the sample was spun in an ultracentrifuge at 90700*g*, 4 °C, for 30 min. The supernatant was diluted 2-fold with distilled water and applied to a 100-mL Ni-NTA-Superflow (Qiagen) column equilibrated with 50 mM HEPES, 0.1% DDM, pH 7.4 (buffer A). The column was washed sequentially with 200 mL of buffer A, 200 mL of 50 mM HEPES, 300 mM NaCl, 0.1% DDM, pH 7.4 (buffer B), and 200 mL of 50 mM HEPES, 20 mM imidazole, 0.1% DDM, pH 7.4 (buffer C). The enzyme was eluted with 50 mM HEPES, 200 mM imidazole, 0.1% DDM, pH 7.4 (buffer D), and concentrated using a Filtron 100-kDa membrane. After two cycles of 20-fold dilution with buffer A and reconcentration, the enzyme was frozen and stored at −80 °C prior to use. Enzyme activity was assayed as described previously (*18*) and showed kinetic parameters comparable to those described therein. On the basis of the criteria established by Moody and co-workers (*22*), the enzyme was predominantly (>80%) in its fast form.

Q_B-Depleted enzyme was obtained by solubilizing the enzyme using 1% TX-100/1% *n*-octyl β-D-glucoside. After ultracentrifugation as above, the supernatant was placed on ice overnight. The mixture was subjected to a second round of ultracentrifugation to remove the remaining cellular debris which had precipitated. The solubilized enzyme was loaded onto the Ni-NTA-Superflow column equilibrated with 50 mM HEPES, 0.1% TX-100, pH 7.4 (buffer E). The enzyme was washed sequentially with 200 mL of 50 mM HEPES, 300 mM NaCl, 0.1% TX-100, pH 7.4 (buffer F), and 200 mL of buffer C. Elution of the enzyme from the column was accomplished using buffer D. The eluted protein was concentrated and frozen as described above, in buffer A.

Freeze-Quench EPR Spectroscopy. A complete description of the freeze-quench technique is given elsewhere (*23*). The freeze-quench EPR experiments were performed using an Update Instruments syringe ram with a model 705A ram controller and a quenching bath containing 8 L of isopentane maintained at −140 °C by an external liquid nitrogen bath. The setup consisted of two syringes, one containing the enzyme (160−200 μM) in buffer A and the other containing UQ_2H_2 in 50 mM HEPES, 0.1% DDM, 5 mM DTT, pH 7.4 (buffer G), or a buffer G blank. The DTT is used to generate the UQ_2H_2 from UQ_2 in situ; it does not react with cytochrome bo_3 itself, and the reduction of the quinone by DTT occurs on a time scale slower than the ∼1 s of reaction time monitored in these reactions. Depending on the reaction, samples were equilibrated under 1 atm of O_2 or 1 atm of Ar on ice for 1 h prior to loading into the syringes. The syringes were equilibrated at 5 °C with an ice−water bath prior to reaction. Reactions were performed by driving the syringe ram at 1 cm s^{-1}. The reagents were combined in a mixing chamber and passed through an aging hose before being sprayed into the liquid isopentane. The frozen crystals which formed were collected in a packing funnel and subsequently packed into the EPR tubes using poly(tetrafluoroethylene)-tipped steel packing rods. The packing factor (ratio of the sample volume to the total volume of frozen sample + isopentane) was estimated to be 70%. The time points measured in the reactions were varied by changing the length of the aging hose.

EPR spectra were taken on a Bruker ER 200D-SRC EPR spectrometer with an Oxford Instruments ESR 910 continuous flow cryostat or on a Varian E-109 EPR spectrometer with an Oxford Instruments ESR-900 cryostat. Spectra were taken at 5 and 70 K. Other instrument settings were as follows: power = 6.3 mW (5 K) or 0.2 mW (70 K), frequency = 9.65 GHz, gain = 8×10^4, modulation frequency = 100 kHz, modulation amplitude = 10 G, time constant = 100 ms, scan time = 200 s. The high-spin heme intensities were measured as the amplitude of the $g_\perp$ signals

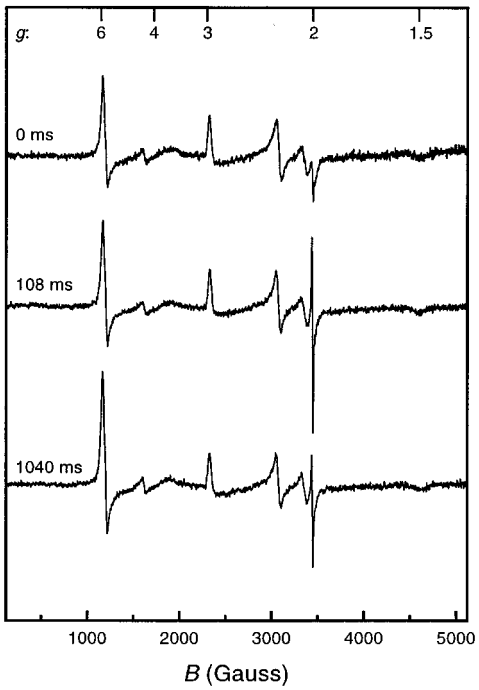

FIGURE 2: EPR spectra of the reaction of 80 μM cytochrome bo_3 with 43 μM UQ_2H_2 under 1 atm of O_2. The spectra were taken at 5 K. Other conditions are given in the text.

at $g = 6$ at 5 K. The low-spin heme was quantitated by the amplitude of the g_y signal ($g = 2.24$) at 5 K. The semiquinone signal intensities were measured as a peak−trough amplitude at 70 K, except for the quantitation against an external flavodoxin standard, where double integration was used.

RESULTS

Reactions of cytochrome bo_3 with UQ_2H_2 were performed with a substrate:enzyme ratio of 1:2, so that a vast majority of those enzyme molecules which reacted with quinol reacted with only 1 equiv. These reactions were monitored using EPR spectroscopy, as described above. Assuming that the lifetime of the Michaelis complex for this reaction is short relative to the diffusion time of the substrate, the distribution of substrate among the enzyme molecules will follow a binomial distribution. Under this limiting assumption, 61% of the enzyme molecules will react with no substrate molecules, 30% will react with one, 7.6% will react with two, and 1.4% of the enzyme molecules will react with three or more substrate molecules. In comparison, a 1:1 substrate:enzyme ratio would result in 37% of the enzyme molecules reacting with no substrate, 37% reacting with one quinol, 18% reacting with two, and 8% reacting with three or more molecules of substrate; the resulting heterogeneity of the enzyme population would complicate the analysis of both electron distribution and flow. If the substrate:enzyme ratio is significantly less than 1:2, not enough enzyme will react to yield observable changes in the resulting EPR spectra.

Figure 2 shows the EPR spectra from the reaction of 43 μM UQ_2H_2 with 80 μM cytochrome bo_3 under 1 atm of O_2, with time points of 0 s, 108 ms, and 1040 ms. The spectrum of resting enzyme (0 ms) shows the high-spin heme o_3 signal at $g = 6$, the rhombic signal from low-spin heme b at $g =$ 3.0, 2.2, and 1.5, and a type 2 copper signal from Cu_B in the region of $g = 2$. Whereas the related cytochrome aa_3 shows strong, antiferromagnetic coupling of the $S = 5/2$ heme and $S = 1/2$ copper center to yield an EPR-silent $S = 2$ species, the binuclear center is partially decoupled in cytochrome bo_3, as evidenced by the respective component EPR signals.[2] The signal at $g = 4.3$ arose from adventitious iron in the sample. At a reaction time of 108 ms, the EPR spectrum showed a sharp signal near the free-electron g value. This signal had a line width of ~11 G and showed unresolved hyperfine splitting. It was identical to that observed in prior redox titrations of the enzyme (*27, 28*) and could thus be assigned as the Q_B semiquinone. Figure 3 (top) shows the intensity of the semiquinone signal at 70 K as a function of time. The semiquinone intensity reached a maximum at 108 ms and decayed to a level about one-half that of its maximum by 1040 ms. Integration of the semiquinone signal against a flavodoxin external standard gave a maximum semiquinone concentration of 22 μM. As the semiquinone signal did not decay back to the baseline, the data were treated with a model depicted in Scheme 1 for the formation and decay of the semiquinone. It assumes the existence of two subpopulations

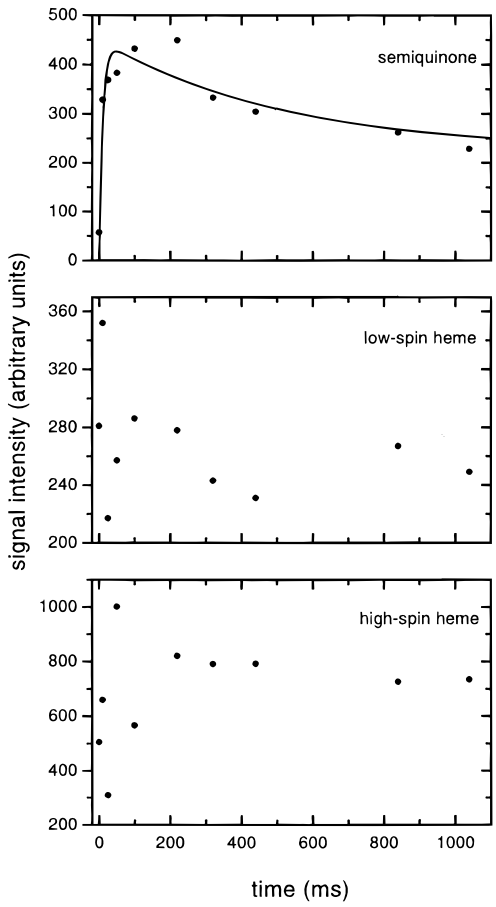

FIGURE 3: Signal intensity of the semiquinone ($Q_B^{\bullet}$, top), low-spin ferric heme (heme b, middle), and high-spin ferric heme (heme o_3, bottom) as a function of time in the reaction of 80 μM cytochrome bo_3 with 43 μM UQ_2H_2 under 1 atm of O_2. The solid line in the upper trace is a fit of the model in Scheme 1 to the semiquinone intensity data.

[2] Decoupling of the heme−copper binuclear center has also been observed in *Bacillus subtilis* aa_3-600 quinol oxidase (*24*), heat-treated bovine cytochrome *c* oxidase (*25*), and the SoxABCD complex in *Sulfolobus acidocaldarius* (*26*). We do not attribute any mechanistic significance to this decoupling.

Scheme 1: Mechanistic Model Used for the Fitting of the Kinetic Data for Semiquinone Formation and Decay, with Associated Rate Constants k_{form} and k_{decay}

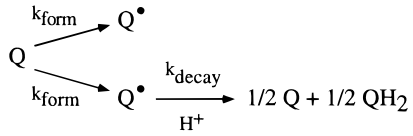

of enzyme indistinguishable in the resting state. Semiquinone formation occurs at a given rate in all of the reacting enyzme molecules. However, in one subpopulation, the semiquinone is stable, while in the other, the semiquinone is subject to disproportionation. This model predicts a monoexponential rise in semiquinone intensity, with an exponential decay to a nonzero value. A fit of this model to the data yielded a formation rate constant of approximately 100 s^{-1} and a decay rate constant of ~2 s^{-1}. A modest degree of uncertainty in these numbers arises from the scatter in the data points.

Figure 3 (middle, bottom) shows the evolution of the low- and high-spin heme signals as a function of time. In both of these plots, the signals show a dramatic scatter over the first 100 ms of reaction time, before reaching a reasonably stable level thereafter. That this scatter did not arise from discrepancies in sample packing is shown by a lack of systematic variation of signal intensity among the semiquinone, high-spin heme, and low-spin heme. At certain time points, the low-spin heme intensity reached levels substantially higher than that at $t = 0$ ms, an unexpected result in light of the fact that heme *b* was fully oxidized at the start of the reaction and hence should have yielded the highest intensity at that point. This behavior was likely due to interference from dioxygen in signal formation, as it was not observed under anaerobic conditions (see below). Any further interpretation is limited by the complexity of these signals.

To isolate the oxidation of quinol from any subsequent dioxygen chemistry, the reaction of cytochrome bo_3 (96 μM) with UQ_2H_2 (48 μM) was performed under 1 atm of argon. Figure 4 shows the evolution of the EPR spectra under these conditions. As with the aerobic reaction, semiquinone formation and decay were prominent. However, a pronounced decrease in the intensity of the low-spin heme signal was also observed, corresponding to heme *b* reduction. In addition, the high-spin heme signal increased in intensity, suggesting that electron donation to the binuclear site primarily resulted in the reduction of Cu_B and the decoupling of the binuclear site. Figure 5 shows the intensity of the semiquinone and heme signals as a function of time. Using the model in Scheme 1, best fits of the data yielded a rate constant of approximately 140 s^{-1} for semiquinone formation and a rate constant of 5 s^{-1} for decay of the species. While these values are nominally higher than those from the identical reaction run under 1 atm of dioxygen, the differences are sufficiently small as to be insignificant, considering the scatter in the data points. The near-equality of semiquinone intensity at maximal production in both cases also testifies to the near-equality of reaction rates. Hence, semiquinone production and decay appear to be independent of any dioxygen chemistry occurring in the enzyme. The heme *b* signal showed a reduction to approximately two-thirds of its maximum value within the dead time of the

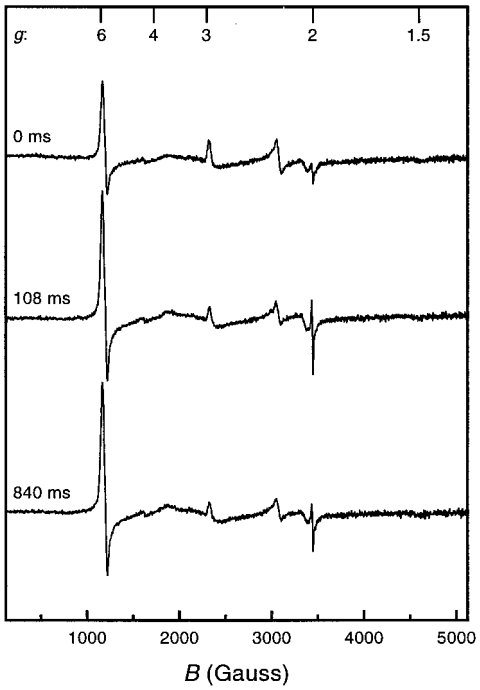

FIGURE 4: EPR spectra of the reaction of 96 μM cytochrome bo_3 with 48 μM UQ_2H_2 under 1 atm of Ar. The spectra were taken at 5 K. Other conditions are given in the text.

experiment. This signal then remained essentially constant over the 1-s time course of the reaction. In a similar fashion, the high-spin heme signal showed a rapid increase in intensity during the dead time of the freeze-quench apparatus, reaching a stable level for the remainder of the observed reaction. This rise in intensity reflects the decoupling of the binuclear center upon reduction of the Cu_B site. Single-exponential fits were made to the heme intensity data in order to calculate reduction levels, and the fits are shown in Figure 5, but the electron-transfer rates were too high to yield meaningful rate constants. A steady-state assay of enzyme activity at 5 °C yielded a k_{cat} for the enzyme of 500 s^{-1}, a value in accord with the rapid reduction of heme *b* and Cu_B. The somewhat slower rate of $Q_B^{\bullet}$ formation can be understood if the electron transfer from $Q_A^{\bullet}$ to Q_B is mediated by heme *b* (see below). Because the formation of $Q_B^{\bullet}$ under single-turnover conditions is slower than k_{cat} determined under steady-state conditions, it cannot be stated unequivocally that the semiquinone is a necessary intermediate in the catalytic cycle. However, the fact that the rates are so close to each other implies that the semiquinone is still important mechanistically. In addition, it should be noted that in a coupled vesicle, the presence of a proton gradient will slow the electron transfers contributing to k_{cat}.

On the basis of integration against a flavodoxin standard, the Q_B semiquinone reached a maximum concentration of 20 μM. Heme *b*, which was fully oxidized upon initiation of the reaction, was reduced to yield 32 μM ferrous heme *b*. The reduction level of the binuclear heme−copper site could not be quantitated directly, as the extent of spin coupling between the two centers was unknown. However, it can be assumed that the electrons not accounted for by the semiquinone and heme *b* resided in the binuclear site. With this assumption, the total concentration of reduced species at the binuclear site was 44 μM. Hence, within the error of the EPR quantitation (approximately 10%), half of the electrons

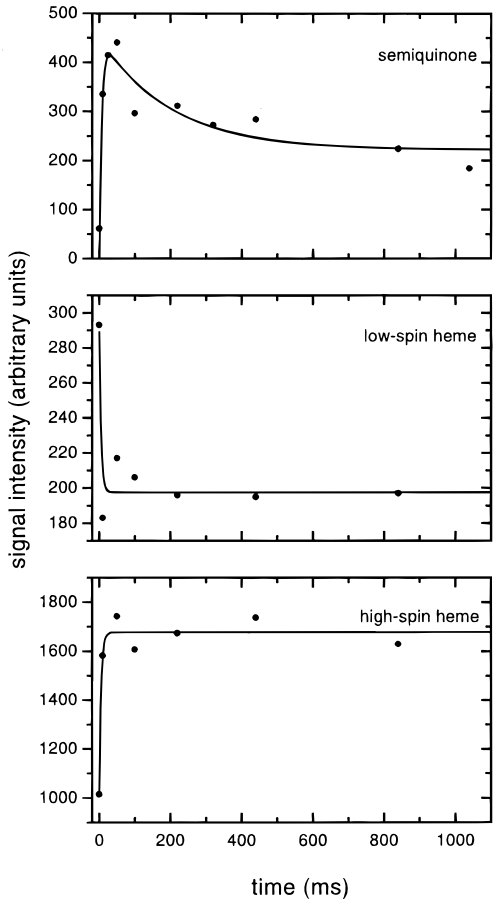

FIGURE 5: Signal intensity of the semiquinone ($Q_B^{\bullet}$, top), low-spin ferric heme (heme *b*, middle), and high-spin ferric heme (heme o_3, bottom) as a function of time in the reaction of 96 μM cytochrome bo_3 with 48 μM UQ_2H_2 under 1 atm of Ar. The fit to the semiquinone data (solid line, top) used the kinetic model in Scheme 1. Single exponentials were used to fit the low- and high-spin heme intensity data.

from the quinol substrate ended up in the Q_B/heme *b* site and half traveled to the heme o_3/Cu_B site. The decay of the semiquinone signal could have arisen from either oxidation to the quinone form or reduction to the quinol form; as neither the heme *b* nor the binuclear center appeared to change during this time, dissociation and disproportionation of the semiquinone is the most likely explanation for the observed decay.

For the reactions of cytochrome bo_3 with UQ_2H_2, under both dioxygen and argon, the power saturation behavior of the semiquinone signal was studied at 70 K with time points of 10, 220, and 1040 ms (O_2) or 10, 108, and 840 ms (Ar). In all cases, the power saturation data could be fit by a single species with $P_{1/2}$ at approximately 160 μW and a homogeneity parameter *b* of about 0.7. The observed value of $b < 1$ is indicative of a substantial dipole−dipole contribution to the spin relaxation (*29*). As Q_B and heme *b* are in close proximity, we assign this species as $Q_B^{\bullet}$ adjacent to ferric heme *b*. By comparison, Ingledew and co-workers (*27*) reported a homogeneous signal for the semiquinone ($b \approx 3$ for the derivative signal) during redox titrations of cytochrome bo_3. This species had a $P_{1/2}$ value of 0.2 mW at 123 K and was assigned as semiquinone adjacent to reduced heme *b*. The finding in this work that the semiquinone exists predominantly in proximity to oxidized heme *b*, despite the high average reduction level of heme *b*, implies that during the time frame measured in these experiments, one and only one electron is shared between Q_B and heme *b*.

The Q_B-depleted form of cytochrome bo_3 has been characterized previously (*5*). To assess the role of the Q_B in the initial electron transfers from the substrate quinol, a sample of this enzyme (86 μM) was reacted with 0.5 equiv of UQ_2H_2 (43 μM) under 1 atm of O_2. Prior analysis of this enzyme showed that it contained approximately 0.3 quinone per enzyme molecule and retained approximately 85% of the activity of native enzyme under multiple-turnover conditions. However, there was no significant change in the EPR spectra of the enzyme over the 1-s time frame of the experiment (data not shown).

A final reaction was performed, using 96 μM cytochrome bo_3 preincubated with 200 μM KCN (final concentrations) and 48 μM UQ_2H_2, to assess the effects of cyanide on electron transfer within the enzyme. Qualitatively, the reaction was the same as the reaction in the absence of cyanide. Most notably, the high-spin signal from heme o_3 was present throughout the reaction. As cyanide binding to oxidized heme will drive the iron into a low-spin state, this result implies that upon reduction of the heme−copper binuclear center, cyanide preferentially bound to Cu_B rather than at heme o_3.

DISCUSSION

In this study, freeze-quench EPR was used to study the reaction of ubiquinol with cytochrome bo_3 under conditions in which the enzyme can react with essentially only one molecule of substrate. The results from signal quantitation and power saturation indicate that the distribution of quinol molecules among the molecules of cytochrome bo_3 is more uniform than one would predict by assuming a binomial distribution. Over the time window of these experiments, one electron from the oxidation of quinol is distributed between Q_B and heme *b*, while the second electron ends up in the heme−copper binuclear site. These results demonstrate a split electron-transfer pathway in the oxidation of quinol, with heme *b* and Cu_B acting as the initial electron acceptors. Because one electron is distributed between the Q_B site and heme *b*, the two centers can be assumed to exist in a quasi-equilibrium and the difference in reduction potentials between the two centers can be inferred.

There have been several studies measuring the reduction potentials of the redox centers in cytochrome bo_3 using redox titrations on either membrane fragments (*30*−*35*) or isolated enzymes (*27*, *28*, *36*−*38*). These studies show a large degree of variability in the observed potentials, because of varied isolation conditions, the presence of cytochrome contaminants, partial replacement of heme *b* with heme *o* in certain overexpressing strains of *E. coli*, difficulty in deconvoluting contributions from the *b* and *o* hemes to overall optical absorption spectra, redox cooperativity, and accidental removal of the quinone from the Q_B site by harsh detergent treatment. Reported heme potentials span the range 55−265 mV. The reduction potentials for Q_B are well-established under titration conditions, with midpoint potentials $E_m = 22$ mV ($Q/Q^{\bullet}$) and 115 mV ($Q^{\bullet}/QH_2$) at pH 7.0 (*27*). From the data of Ingledew and co-workers (*27*), the potentials at pH 7.4 can be estimated as 14 and 82 mV. Interpolation of the data of Sato-Watanabe and co-workers (*28*) gives values of

approximately 0 and 115 mV. These differences are minor, and most likely reflect slightly different preparatory methods. Literature values for the copper potential range from 350 to 408 mV, making it the most easily reducible center in the enzyme. It should be noted that the conditions of the redox titration are nonphysiological, such that redox cooperativity under turnover conditions can alter these potentials. In particular, in the presence of oxidized heme *b*, the Q_B semiquinone anion may have an additional stabilization due to electrostatic interactions, driving the two reduction potentials closer together. For the purposes of this discussion, values of 14 mV ($Q/Q^{\bullet}$) and 82 mV ($Q^{\bullet}/QH_2$) are used for the quinone at the Q_B site.

The relative reduction potential of heme *b* with respect to Q_B under turnover conditions can be calculated by assuming that the electron distribution between Q_B and heme *b* is an equilibrium distribution, that the temperature dependence of the Q_B and heme *b* potentials is the same over the range between room temperature and the temperature at which the sample freezes, and that for the majority of enzyme molecules which have reacted with quinol, one electron is distributed between heme *b* and Q_B. The first assumption is not strictly true, as the decay of semiquinone signal is not accompanied by a decrease in ferrous heme *b* concentration; however, any errors associated with this assumption would yield an overestimate of the heme *b* potential. The second assumption is likely valid, as an electron transfer between the two centers should not have a significant entropic component, and the third assumption is verified on the basis of the power saturation data given above. By using the concentrations of semiquinone (20 μM) and ferrous heme *b* (32 μM) at 50 ms, a difference of 12 mV between the $Q/Q^{\bullet}$ and heme *b* potentials is obtained through the application of the Nernst equation. This gives rise to an approximate value of 30 mV for the reduction potential of heme *b*. However, if the decay of the semiquinone signal represents a slow approach to an equilibrium in which the semiquinone concentration is approximately one-half that at 50 ms, a heme potential of about 45 mV is obtained. If one assumes a binomial distribution of quinols among the enzyme molecules, with the condition that no more than two quinol molecules can react with one enzyme molecule, 34% of the molecules react with one quinol and 8% with two. Under this assumption, the reduction potential of the heme *b* increases by only 5−10 mV. Hence, the reduction potential of heme *b* can be estimated at between 30 and 60 mV. It is worth noting that such low values have been reported in the literature on the basis of redox titrations (*28*, *38*).

In the freeze-quench experiments, the potential of heme o_3 could not be determined directly because of the high reduction potential of Cu_B and the coupling of the binuclear site. However, redox titrations at near-physiological pH have placed the potential in the range of 123−265 mV. While this range is large, it is clear that the potential is much greater than that for heme *b* and significantly less than that for Cu_B.

The relative reduction potentials of Q_B, heme *b*, and heme o_3 have three important implications with regard to possible proton translocation mechanisms. First, a low heme *b* potential implies that electron transfers from substrate quinol to Q_B and heme *b*, as proposed for a cytochrome *c* oxidase-type proton pump, would be thermodynamically unfavorable, as the two-electron reduction potential of membrane-bound quinones has been estimated as 60−70 mV (*39*, *40*). Second, as the $Q_A/Q_A^{\bullet}$ potential must be significantly lower than 60 mV in order to allow electron transfer to heme *b*, and ultimately to form $Q_B^{\bullet}$, the $Q_A^{\bullet}/Q_AH_2$ potential must be correspondingly higher than 60 mV. Thus, one must have a redox center (e.g., Cu_B) with a much higher redox potential than heme *b* in order to drive the first electron transfer from Q_AH_2 into the enzyme. Third, the preferential reduction of heme *b* over heme o_3, despite the higher reduction potential of heme o_3, suggests a kinetic barrier to electron transfer between the hemes, again unexpected if one assumes proton pumping analogous to that in cytochrome *c* oxidase. In contrast, these three observations are predicted by a Q-cycle model. A more detailed treatment of the thermodynamics of electron transfer through cytochrome bo_3 will be presented elsewhere.

Two other observations from this work appear to favor a Q-cycle over the ion-pump model of proton translocation. Cu_B is reduced more rapidly than Q_B, such that $Q_B^{\bullet}$ cannot be an intermediate in the reduction of Cu_B. Also, the equal distribution of electrons between the Q_B/heme *b* centers and the heme−copper center, along with the observation that heme *b* and Cu_B are the first centers reduced, is indicative of a split electron-transfer pathway, as envisioned in the Q-cycle model. As proton translocation is tightly coupled to electron transfers, the differences in electron transfer between cytochrome bo_3 and cytochrome *c* oxidase suggest that the proton translocation mechanisms of the two enzymes are not, in fact, identical.

That a substantial kinetic barrier to electron transfer from heme *b* to heme o_3 exists in cytchrome bo_3 was not altogether expected. Studies on the related cytochrome *c* oxidase, in which photolysis of the CO-mixed-valence form of the enzyme was used to induce intramolecular electron transfer, yielded electron-transfer rates of 2×10^5 s^{-1} between heme *a* and heme a_3 (*41*). In bovine cytochrome *c* oxidase, hemes *a* and a_3 are ligated by residues H378 and H376, respectively. These two histidines lie on roughly opposite sides of helix X in this enzyme, but the geometries of the hemes are such that they come within 5 Å of each other at the periphery of the porphyrin planes (*42*), suggesting a facile electron-transfer pathway between the two hemes. In cytochrome bo_3, mutagenesis studies (*43*−*45*) have revealed that the analogous residues H419 and H421 bind heme o_3 and heme *b*, respectively, suggesting a similarity of structure and hence a similarly rapid electron-transfer rate. Studies on the photolysis of CO-mixed-valence cytochrome bo_3 (*46*) revealed a rapid electron transfer to heme *b* from heme *o* upon dissociation of the bound CO; however, the conditions used to isolate the enzyme are similar to those reported for the removal of the quinone from the Q_B site. A perturbation in the heme *b* environment upon removal of the Q_B has been shown by optical spectroscopy (*5*); the extent to which this affects the geometry of heme *b* with respect to heme o_3 has yet to be determined. In contrast, resonance Raman studies of the reaction of fully reduced, CO-bound cytochrome bo_3 with dioxygen under flow-flash conditions (*47*) have revealed only a slow oxidation of heme *b*, with a rate constant of 1 s^{-1} for this process. Other flow-flash studies have revealed two or three kinetic phases in the reaction of cytochrome bo_3 with dioxygen (*8*, *48*−*50*), some of which are attributed to rapid (700−50000 s^{-1}) oxidation of heme *b*. These phases

are not well-characterized, and the state of the enzyme, particularly with regard to quinone content, is not always clear. In the present study, the enzyme is known to be intact, and hence a kinetic barrier is likely to be present under physiological conditions.

Interpretations of the flow-flash experiments have been limited by the assumption that an ion-pump mechanism occurs in cytochrome bo_3 and hence that the only electron sink in the enzyme is the binuclear dioxygen reduction site. Under a Q-cycle mechanism, oxidation of heme *b* would correspond to electron transfer to Q_B, not to the heme−copper site. In addition, if Q_B is fully reduced at the start of the reaction, it would be able to dissociate and act as an electron donor at the Q_A site as the reaction with dioxygen proceeds, leading to an additional kinetic phase. Thus, if reduction of dioxygen to a state more reduced than peroxide occurs under flow-flash conditions, the origin of the additional electrons cannot be determined unequivocally.

In cytochrome *c* oxidase, the electron transfers coupled to proton pumping occur when the enzyme is in its two- and three-electron-reduced states (i.e., the peroxidic and oxyferryl forms). While the experiments in this work do not involve the analogous forms of cytochrome bo_3, the results herein place limitations on the subsequent chemistry. Prior to binding of dioxygen, the enzyme appears to operate via a Q-cycle, releasing four protons from the oxidation of two quinol molecules. Upon dioxygen binding to the two-electron-reduced heme−copper center, the reduction potential of the binuclear site increases by at least 500 mV. This increase in potential may serve to change the electron-transfer pathways in the enzyme. However, the subsequent electron transfers must be coupled to the translocation of four protons, based on the observed $8H^+/4e^-$ stoichiometry over the entire reaction cycle of this enzyme. At least two of the remaining protons must be released as a direct result of quinol oxidation. The remaining two protons could be translocated either by a repeat of the Q-cycle or by ion pumping. Note that in the latter case, only a 1:1 H^+:e^- stoichiometry would be observed for the last two electrons, rather than the 2:1 ratio observed in the cytochrome *c* oxidases. Hence, even if an ion-pump mechanism occurs as part of the reaction cycle, its characteristics must be different from those of the cytochrome *c* oxidases. From the standpoint of simplicity, the operation of a Q-cycle over the entire cycle of enzyme turnover is preferable to a combined Q-cycle/ion-pump mechanism, given the same proton translocation stoichiometry.

If the removal of quinone from the enzyme changes the electron-transfer rates between heme *b* and heme o_3, one must address the issue of electron transfer into cytochrome bo_3 during the time when no quinone is bound. The Q_B-depleted enzyme is capable of catalyzing quinol oxidation at a rate 85−90% of that of native enzyme. This may result from reconstitution of the Q_B site with the small amount of UQ_2 present in the quinol samples utilized in the turnover assays or from an alternative electron-transfer pathway not involving Q_B. As the freeze-quench results suggest that heme *b* and Cu_B act as the initial electron acceptors, either of these two scenarios is feasible. In the freeze-quench reaction of Q_B-depleted enzyme, the lack of change in the EPR signals may suggest that no electron transfer occurs. However, if electron transfer from heme *b* to the binuclear site can occur within the dead time of the freeze-quench apparatus when no Q_B is present, no change in the heme *b* EPR signal would be observed. In addition, a two-electron reduction of the heme−copper binuclear site is not likely to induce a significant change in the heme o_3 signal, as a large fraction of the heme−copper sites are EPR-silent in the oxidized state because of *J* coupling. This second possibility is more in accord with the known reactivity of the enzyme. In the context of the Q-cycle model, Q_B appears to be acting as a sort of electron gate, accepting electrons when present but allowing a leak of electrons to the heme−copper site when absent. Further experiments are in progress to clarify the freeze-quench data and to understand the role of Q_B in mediating the electron transfer in this enzyme.

CONCLUSION

The use of freeze-quench EPR spectroscopy, with its ability to assay the oxidation states of all of the redox centers in cytochrome bo_3, has allowed an analysis of the electron transfers in this enzyme. The rapid reduction of heme *b* and Cu_B upon reaction with quinol, the electron distribution within the enzyme, and a substantial kinetic barrier to electron transfer from heme *b* to the higher-potential heme o_3 site suggest the operation of a Q-cycle mechanism, whereas the low potentials of Q_B and heme *b*, along with the kinetic barrier to heme o_3 reduction, suggest that the electron transfers predicted in a cytochrome *c* oxidase-type ion-pump model are not viable. Any ion-pump model postulating electron transfers other than those presented in this work must explain the involvement of Q_B in the reaction cycle, especially the fact that it is not a primary electron acceptor; to date, no other models have been presented. As with other enzymes involved in bioenergetics, the activity of cytochrome bo_3 is modulated by subtle interactions between the various redox centers within the protein. In particular, both Q_A and Q_B appear to be crucial in directing electron transfer through the protein. The presence or absence of Q_B clearly has an influence on CO-flow-flash experiments, and interaction between the two quinone binding sites has been deduced previously.

The grouping of the quinol oxidases and cytochrome *c* oxidases into a single superfamily is primarily based on the structural similarity of subunit I in these enzymes. The existence of a Q-cycle mechanism in the quinol oxidases would suggest that subunit I is a conserved subunit solely on account of its dioxygen reduction capability, and the interaction of this subunit with other redox centers and subunits in the enzyme ultimately determines the means by which these enzymes couple the reduction of dioxygen with proton translocation. It is of particular interest that the low-spin heme in subunit I appears to be able to take on different electron-transfer roles in the quinol oxidases and cytochrome *c* oxidases, despite the known structural similarities in these enzymes. The much lower potential (∼50 mV) of heme *b* in cytochrome bo_3 as compared to that of heme *a* in cytochrome aa_3 (∼290 mV) explains the ability of cytochrome bo_3 to reduce Q_B. Other quinol oxidases, however, possess a low-spin heme *a* in place of heme *b* (*1*). How these enzymes operate, in terms of both electron transfer and proton translocation, should provide further insight into the functional and evolutionary relationships among the various enzymes in the heme−copper oxidase family.

ACKNOWLEDGMENT

We would like to thank Siegfried Musser, Robert Gennis, and Jeffrey Osborne for insightful comments, Michael Stowell for the synthesis and purification of the UQ_2 used in this work, and Kirk Hansen for experimental assistance.

REFERENCES

1. García-Horsman, J. A., Barquera, B., Rumbley, J., Ma, J., and Gennis, R. B. (1994) *J. Bacteriol. 176*, 5587−5600.
2. Malatesta, F., Antonini, G., Sarti, P., and Brunori, M. (1995) *Biophys. Chem. 54*, 1−33.
3. Musser, S., Stowell, M. H. B., and Chan, S. I. (1995) *Adv. Enzymol. 71*, 79−208.
4. Chepuri, V., Lemieux, L., Au, D. C.-T., and Gennis, R. B. (1990) *J. Biol. Chem. 265*, 11185−11192.
5. Sato-Watanabe, M., Mogi, T., Ogura, T., Kitagawa, T., Miyoshi, H., Iwamura, H., and Anraku, Y. (1994) *J. Biol. Chem. 269*, 28908−28912.
6. Puustinen, A., Finel, M., Virkki, M., and Wikström, M. (1989) *FEBS Lett. 249*, 163−167.
7. Babcock, G. T., and Varotsis, C. (1993) *J. Bioenerg. Biomembr. 25*, 71−80.
8. Svensson, M., and Nilsson, T. (1993) *Biochemistry 32*, 5442−5447.
9. Hirota, S., Mogi, T., Ogura, T., Hirano, T., Anraku, Y., and Kitagawa, T. (1994) *FEBS Lett. 352*, 67−70.
10. Verkhovsky, M. I., Morgan, J. E., Puustinen, A., and Wikström, M. (1996) *Biochemistry 35*, 16241−16246.
11. Morgan, J. E., Verkhovsky, M. I., Puustinen, A., and Wikström, M. (1995) *Biochemistry 34*, 15633−15637.
12. Moody, A. J., Rumbley, J. N., Ingledew, W. J., Gennis, R. B., and Rich, P. R. (1993) *Biochem. Soc. Trans. 21*, 255S.
13. Moody, A. J., and Rich, P. R. (1994) *Eur. J. Biochem. 226*, 731−737.
14. Watmough, N. J., Cheesmen, M. R., Greenwood, C., and Thomson, A. J. (1994) *Biochem. J. 300*, 469−475.
15. Brittain, T., Little, R. H., Greenwood, C., and Watmough, N. J. (1996) *FEBS Lett. 399*, 21−25.
16. Hallén, S., Svennson, M., and Nilsson, T. (1993) *FEBS Lett. 325*, 299−302.
17. Musser, S. M., Stowell, M. H. B., and Chan, S. I. (1993) *FEBS Lett. 327*, 131−136.
18. Musser, S. M., Stowell, M. H. B., Lee, H. K., Rumbley, J. N., and Chan, S. I. (1997) *Biochemistry 36*, 894−902.
19. Hill, B. C. (1993) *J. Bioenerg. Biomembr. 25*, 115−120.
20. Trumpower, B. L. (1990) *Microbiol. Rev. 54*, 101−129.
21. Brandt, U., and Trumpower, B. (1994) *Crit. Rev. Biochem. Mol. Biol. 29*, 165−197.
22. Moody, A. J., Cooper, C. E., Gennis, R. B., Rumbley, J. N., and Rich, P. R. (1995) *Biochemistry 34*, 6838−6846.
23. Ballou, D. P. (1978) *Methods Enzymol. 54*, 85−93.
24. Fann, Y. C., Ahmed, I., Blackburn, N. J., Boswell, J. S., Verkhovskaya, M. L., Hoffman, B. M., and Wikström, M. (1995) *Biochemistry 34*, 10245−10255.
25. Musser, S. M., Fann, Y.-C., Gurbiel, R. J., Hoffman, B. M., and Chan, S. I. (1997) *J. Biol. Chem. 272*, 203−209.
26. Gleissner, M., Kaiser, U., Antonopoulos, E., and Schäfer, G. (1997) *J. Biol. Chem. 272*, 8417−8426.
27. Ingledew, W. J., Ohnishi, T., and Salerno, J. C. (1995) *Eur. J. Biochem. 227*, 903−908.
28. Sato-Watanabe, M., Itoh, S., Mogi, T., Matsuura, K., Miyoshi, H., and Anraku, Y. (1995) *FEBS Lett. 374*, 265−269.
29. Galli, C., Innes, J. B., Hirsh, D. J., and Brudvig, G. W. (1996) *J. Magn. Reson. 110*, 284−287.
30. Reid, G. A., and Ingledew, W. J. (1979) *Biochem. J. 182*, 465−472.
31. Hackett, N. R., and Bragg, P. D. (1983) *J. Bacteriol. 154*, 708−718.
32. Lorence, R. M., Green, G. N., and Gennis, R. B. (1984) *J. Bacteriol. 157*, 115−121.
33. Salerno, J. C., Bolgiano, B., and Ingledew, W. J. (1989) *FEBS Lett. 247*, 101−105.
34. Salerno, J. C., Bolgiano, B., Poole, R. K., Gennis, R. B., and Ingledew, W. J. (1990) *J. Biol. Chem. 265*, 4364−4368.
35. Bolgiano, B., Salmon, I., and Poole, R. K. (1993) *Biochim. Biophys. Acta 1141*, 95−104.
36. Kita, K., Konishi, K., and Anraku, Y. (1984) *J. Biol. Chem. 259*, 3368−3374.
37. Withers, H. K., and Bragg, P. D. (1990) *Biochem. Cell Biol. 68*, 83−90.
38. Bolgiano, B., Salmon, I., Ingledew, W. J., and Poole, R. K. (1991) *Biochem. J. 274*, 723−730.
39. Ohnishi, T., and Trumpower, B. L. (1980) *J. Biol. Chem. 255*, 3278−3284.
40. Rich, P. R. (1984) *Biochim. Biophys. Acta 768*, 53−79.
41. Verkhovsky, M. I., Morgan, J. E., and Wikström, M. (1992) *Biochemistry 31*, 11860−11863.
42. Tsukihara, T., Aoyama, H., Yamashita, E., Tomizaki, T., Yamaguchi, H., Shinzawa-Itoh, K., Nakashima, R., Yaono, R., and Yoshikawa, S. (1995) *Science 269*, 1069−1074.
43. Minagawa, J., Mogi, T., Gennis, R. B., and Anraku, Y. (1992) *J. Biol. Chem. 267*, 2096−2104.
44. Lemieux, L. J., Calhoun, M. W., Thomas, J. W., Ingledew, W. J., and Gennis, R. B. (1992) *J. Biol. Chem. 267*, 2105−2113.
45. Tsubaki, M., Mogi, T., Hori, H., Hirota, S., Ogura, T., Kitagawa, T., and Anraku, Y. (1994) *J. Biol. Chem. 269*, 30861−30868.
46. Morgan, J. E., Verkhovsky, M. I., Puustinen, A., and Wikström, M. (1993) *Biochemistry 32*, 11413−11418.
47. Wang, J., Rumbley, J., Ching, Y.-C., Takahashi, S., Gennis, R. B., and Rousseau, D. L. (1995) *Biochemistry 34*, 15504−15511.
48. Orii, Y., Mogi, T., Kawasaki, M., and Anraku, Y. (1994) *FEBS Lett. 352*, 151−154.
49. Orii, Y., Mogi, T., Sato-Watanabe, M., Hirano, T., and Anraku, Y. (1995) *Biochemistry 34*, 1127−1132.
50. Puustinen, A., Verkhovsky, M. I., Morgan, J. E., Belevich, N. P., and Wikström, M. (1996) *Proc. Natl. Acad. Sci. U.S.A. 93*, 1545−1548.

BI971714Y